Journal of Alloys and Compounds 504 (2010) 146–150

Contents lists available at ScienceDirect

Journal of Alloys and Compounds

journal homepage: www.elsevier.com/locate/jallcom

Temperature dependency and carrier transport mechanisms of Ti/p-type InP Schottky rectifiers

V. Janardhanam[a], Hoon-Ki Lee[b], Kyu-Hwan Shim[b], Hyo-Bong Hong[c], Soo-Hyung Lee[c], Kwang-Soon Ahn[d], Chel-Jong Choi[a,b,*]

[a] Department of BIN Fusion Technology, Chonbuk National University, Jeonju 561-756, Republic of Korea
[b] School of Semiconductor and Chemical Engineering, Semiconductor Physics Research Center (SPRC), Chonbuk National University, Jeonju 561-756, Republic of Korea
[c] Future Technology Research Group, Electronics and Telecommunications Research Institute (ETRI), Daejeon 305-700, Republic of Korea
[d] School of Display and Chemical Engineering, Yeungnam University, Gyeongsan 712-749, Republic of Korea

ARTICLE INFO

Article history:
Received 30 December 2009
Received in revised form 7 May 2010
Accepted 15 May 2010
Available online 31 May 2010

Keywords:
Schottky contacts
I–V–T characteristics
InP
Ti
Frenkel–Poole emission
Schottky emission

ABSTRACT

We have investigated the temperature dependent current–voltage (*I–V*) characteristics of Ti Schottky contacts to p-type InP. The Ti/p-type InP Schottky diode yielded an ideality factor of 1.08 showing good rectifying behavior with a barrier height of 0.73 eV at 300 K. The capacitance–voltage (*C–V*) characteristics of the Ti Schottky contact to p-type InP have been measured at room temperature and at different frequencies. The barrier heights from *C–V* measurements are calculated to be 0.71, 0.72 and 0.77 eV at 10 kHz, 100 kHz and 1 MHz, respectively. The discrepancy of barrier heights obtained from *I–V* at 300 K and *C–V* characteristics measured at $f = 1$ MHz at 300 K is negligible due to homogenous nature of Schottky diode structures. The characteristic energy of the diode at 300 K showed thermionic emission to be the dominating current mechanism. The analysis of the reverse current–voltage characteristics of the Ti Schottky contact to p-type InP reveals that the main process involved in leakage current could be associated with the Frenkel–Poole emission at 300 K, while at 350 K and 400 K, the Schottky emission.

1. Introduction

The advancement in the semiconductor technology has exposed indium phosphide (InP) as a potential material for the development of optoelectronic and high-speed devices [1]. Over the past few decades, metal–semiconductor (MS) contacts are one of the most widely used rectifiers in the microelectronics industry [2,3]. The fabrication of these MS structures plays a crucial role in developing some useful devices in technology [4]. Due to the technological importance of Schottky junctions, a full understanding of the nature of their electrical characteristics is required [5–7]. Furthermore, the detailed knowledge about the dependence of Schottky diode characteristics on temperature is substantially important for practical applications and for understanding the current conduction mechanisms involved [8]. Previously, many attempts have been made to investigate the electrical properties of InP Schottky diodes. Ejderha et al. [9] studied the current–voltage (*I–V–T*) characteristics of the sputtered Co/p-type InP Schottky diodes in the temperature range of 80–400 K. They observed a double Gaussian distribution before making the correction in current–voltage (*I–V*) characteristics for the effect of the interfacial layer which was attributed to the presence of rough and high resistivity-thin native oxide layer which contains many contacts with low barrier height at the interface and after correction, the barrier height obeyed the single Gaussian distribution model. Singh et al. [10] demonstrated that the soft reverse current–voltage (I_r–V_r) characteristics of Au/p-type InP Schottky diodes with a thin interface layer were well described by the interface layer thermionic emission theory proposed by Wu [11]. Aydogan et al. [12] investigated the *I–V* and capacitance–voltage (*C–V*) characteristics of polypyrrole/p-type InP structures fabricated using electrochemical polymerization of the organic polypyrrole onto the InP substrate. They showed that the discrepancy between barrier heights obtained from *I–V* and *C–V* measurements could be associated with spatial distribution of barrier heights caused by the presence of an interface layer and the inhomogeneities of barrier height at the interface between polypyrrole and InP. Janardhanam et al. [13] investigated *I–V* and *C–V* characteristics of Mo/n-type InP Schottky diodes in the temperature range of 200–400 K. They observed the strong dependence of barrier height and ideality factor on temperature and analyzed the *I–V* characteristics on the basis of thermionic emission theory and the assumption of Gaussian distribution of

* Corresponding author at: School of Semiconductor and Chemical Engineering, Semiconductor Physics Research Center (SPRC), Chonbuk National University, Jeonju 561-756, Republic of Korea. Tel.: +82 63 2703365; fax: +82 63 2703585.
E-mail address: cjchoi@chonbuk.ac.kr (C.-J. Choi).

0925-8388/$ – see front matter © 2010 Elsevier B.V. All rights reserved.
doi:10.1016/j.jallcom.2010.05.074

barrier heights due to barrier inhomogeneities that prevail at the metal–semiconductor interface. Despite these efforts, however, the detailed knowledge of carrier transport mechanisms in InP Schottky rectifiers remains still unclear. In this work, Ti has been used as Schottky contact metal because of its low work function that can yield Schottky contacts with high barrier heights for p-type semiconductors. The temperature dependence of the *I–V* characteristics gives a better understanding of the conduction mechanism and allows one to understand different aspects that shed light on the validity of various processes involved. At low temperatures, electrons are able to surmount the lower barriers and therefore current transport will be dominated by current flowing through the patches of lower Schottky barrier height and a large ideality factor. Generally, low temperature measurements are effective in revealing the current transport mechanism especially for tunneling and the effects of inhomogeneity. Many researchers carried out the temperature dependency of *I–V* and *C–V* characteristics at high temperatures (>300 K) to associate the physical phenomena of the current conduction mechanism occurring in the devices [14–16]. This implies that high temperature is also of importance in effectively understanding the carrier transport mechanism of Schottky barrier diodes. In our study, we investigated the current dependence on the reverse bias voltage above room temperatures.

In this work, the *I–V* characteristics of Ti/p-type InP Schottky diodes have been investigated in the temperature range (300–400 K) in steps of 50 K, and *C–V* characteristics have been measured at different frequencies at room temperature. The dependence of the leakage current on electric field at different temperatures has been presented.

2. Experimental details

Lightly zinc doped p-type InP (1 0 0) wafers with a resistivity of 0.44–0.58 Ω cm given by the manufacturer were used in this work. Before making the contacts, the p-InP wafer was dipped in $5H_2SO_4 + H_2O_2 + H_2O$ solution for 1 min to remove surface damage layer and undesirable impurities. The InP wafers are dipped in HF:H_2O (1:10) solution to remove native oxides from the surface and finally the wafer was rinsed in deionized (DI) water for 30 s. After removing native oxide, 50-nm thick Pt films are evaporated on the back side of the p-type InP, followed by thermal annealing at 350 °C for 1 min in N_2 atmosphere. For Schottky contacts, 30-nm thick Ti and 30-nm thick Ni films are sequentially deposited using e-beam evaporator under a vacuum of 7×10^{-7} Torr. Ni films were used as a capping layer in order to minimize the contamination of Ti Schottky metal films. The Schottky contacts were defined with an area of 300 μm × 300 μm using lift-off lithography. 60 Schottky barrier diodes have been fabricated and characterized. All of them showed alike *I–V* and *C–V* behaviors. *I–V* and *C–V* measurements are carried out using HP4155 parameter analyzer and HP4284A precision LCR meter, respectively.

3. Results and discussion

Fig. 1 shows the current density–voltage (*J–V*) characteristics of Ti/p-type InP Schottky diodes at temperatures in the range of 300–400 K. It is clear that the forward current through the diodes increase with increasing temperature. The reverse current increases with the increase of applied voltage at 300 K, and however, at 350 K and 400 K, the weaker is the voltage dependence. It can be seen that the *I–V* characteristics depend strongly on temperature. For example, the forward and reverse current densities increase with increasing temperatures. This implies that both temperature and voltage can give a significant effect on the carrier transport through Schottky contact between Ti and p-type InP. The diode showed good rectifying behavior at all temperatures. According to thermionic emission theory, the variation of current density with the applied voltage is given by [2,17]:

$$J = J_0 \exp\left(\frac{qV}{nkT}\right)\left[1 - \exp\left(\frac{-qV}{kT}\right)\right] \quad (1)$$

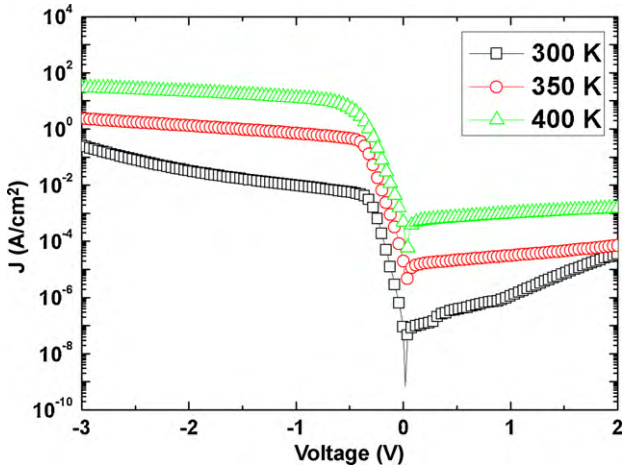

Fig. 1. *J–V* characteristics of Ti/p-type InP Schottky diode in the temperature range of 300–400 K.

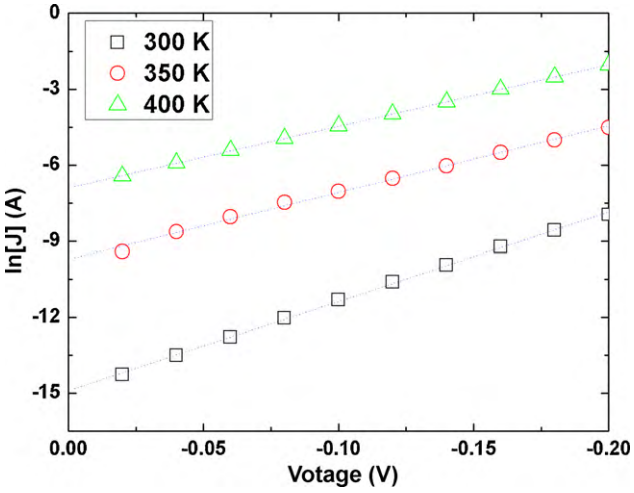

Fig. 2. ln(*J*)–*V* plot of Ti/p-type InP Schottky diode in the temperature range of 300–400 K.

where J_0, the saturation current density given by

$$J_0 = A**T^2 \exp\frac{q\Phi_{b0}}{kT} \quad (2)$$

q: electron charge, *V*: applied voltage, *k*: Boltzmann constant, *n*: ideality factor, A^{**}: Richardson constant (60 A/(cm^2 K^{-2})), *T*: temperature, and Φ_{b0}: barrier height. A plot of ln(*J*) against *V* (Fig. 2) yields J_0 as the intercept at *V* = 0 V. Once J_0 is determined, the barrier height (Φ_{b0}) can be evaluated using

$$\Phi_{b0} = \frac{kT}{q}\ln\left(\frac{A**T^2}{J_0}\right) \quad (3)$$

n, which is a dimensionless parameter and is a measure of the conformity of the diode to pure thermionic emission, can be determined from the slope of the straight line region of the forward bias ln*J–V* shown in Fig. 2 using:

$$n = \frac{q}{kT}\left(\frac{dV}{d(\ln J)}\right) \quad (4)$$

The barrier heights for hole are measured to be 0.73, 0.74 and 0.76 eV for 300 K, 350 K and 400 K, respectively. The diode at 300 K shows ideal behavior with a value of *n* = 1.08. However the diode is deviating from ideality with increase of temperature with minute variation. The values of barrier heights and ideality factor at different temperatures are represented in Table 1. The barrier

Table 1
The experimentally obtained barrier heights and ideality factors of Ni/Ti/p-InP at different temperatures.

Temperature (K)	Barrier height (Φ_{b0}) (eV)	Ideality factor 'n'
300	0.73	1.08
350	0.74	1.18
400	0.76	1.16

height increases with increase of temperature. As the temperature increases, more and more carriers have sufficient energy to surmount the higher barriers. As a result, the dominant barrier height will increase with the temperature and bias voltage. The diodes showed nearly ideal behavior at all temperatures with an ideality factor of 1.08 at 300 K with a barrier height of 0.73 eV. These values are comparable to the values reported by Asubay et al. for Ti/p-InP Schottky diodes at 300 K where the low and high barrier heights are obtained as 0.69 and 0.92 eV and the ideality factors as 1.12 and 1.16 for the identically prepared diodes on the same sample [18].

The C–V measurements can be used to determine the interface quality as well as Schottky barrier height. Fig. 3 shows the forward and reverse bias C–V characteristics of Ti/p-InP Schottky structures measured with different frequencies at room temperature (T = 300 K). It is clear that the capacitance is low at high frequencies (100 kHz, 1 MHz as observed from Fig. 3) and high at low frequency of 10 kHz. Usually, there are various kinds of states at the semiconductor interface [12]. The capacitance is high at low frequencies because all the interface states are affected by the applied signal and are able to give up and accept charges in response to this signal. The interface state capacitance appears directly in parallel with the depletion capacitance and results in a higher total value of the capacitance at low frequencies. At high frequencies, the capacitance is low since the interface state charges do not contribute to the diode capacitance. The depletion layer capacitance per unit area can be expressed as [17]:

$$\frac{1}{C^2} = \left(\frac{2}{\varepsilon_s q N_A A^2}\right)\left(V_{bi} - \frac{kT}{q} - V\right) \quad (5)$$

where V_{bi} is built-in potential. N_A, A, and ε_s are carrier concentration, area of the Schottky contact, and the permittivity of the semiconductor ($\varepsilon_s = 12.5\varepsilon_o$), respectively. Fig. 4 shows the reverse bias C^{-2}–V characteristics for different frequencies measured at 300 K. The x-intercept of the plot of $(1/C^2)$ versus V gives V_o. The V_o is related to V_{bi} by the equation $V_{bi} = V_o + kT/q$, where T is the absolute temperature. The barrier height $\Phi_{(C-V)}$ is given by the equation $\Phi_{(C-V)} = V_{bi} + V_n$, where $V_n = (kT/q)\ln(N_V/N_A)$. The density of states in

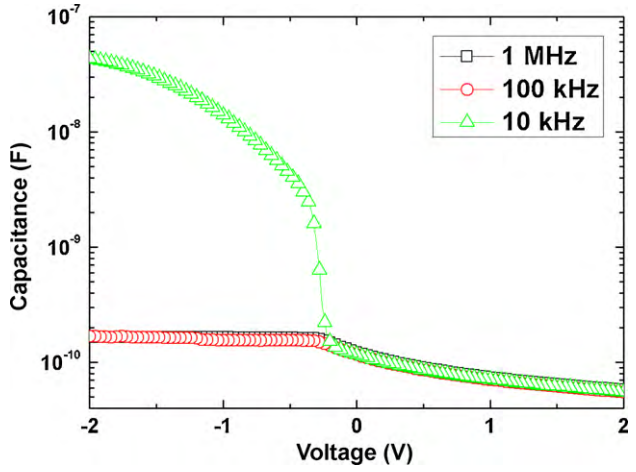

Fig. 3. Capacitance–voltage (C–V) characteristics of Ti/p-type InP Schottky diode at different frequencies at room temperature.

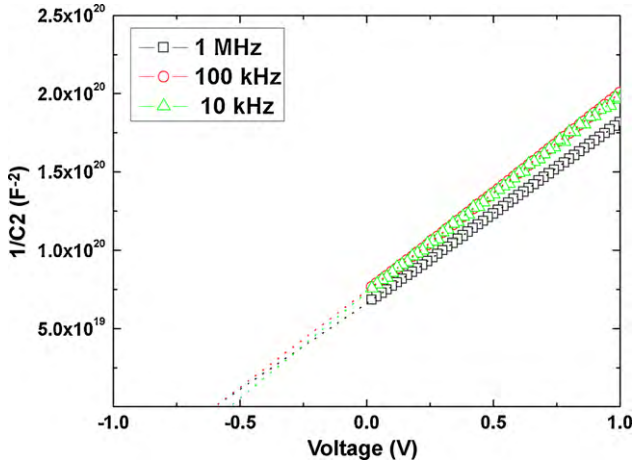

Fig. 4. The reverse bias $1/C^2$–V characteristics of Ti/p-InP Schottky diode at different frequencies at room temperature.

the valence band edge is given by $N_V = 2(2\pi m \times KT/h^2)^{3/2}$, where $m^* = 0.078m_o$ and $N_V = 1.1 \times 10^{19}$ cm^{-3} for InP at room temperature [12,19]. The barrier height values are calculated from C–V measurements at room temperature for different frequencies and are 0.71, 0.72 and 0.77 eV at 10 kHz, 100 kHz, and 1 MHz frequencies, respectively. The barrier height obtained from the I–V characteristics at 300 K is lower than that obtained from C–V characteristics at proper high frequency of f = 1 MHz which is measured at same temperature of 300 K since the C–V method averages over the whole area and measures Schottky barrier diode, whereas the barrier height extracted from the I–V method includes any barrier lowering effect due to the interfacial oxide layer or the interface states and yields an effective barrier height. However, the discrepancy between the barrier height obtained at room temperature (300 K) from C–V measurement at a proper high frequency of f = 1 MHz and the I–V barrier height obtained at 300 K is very small and negligible. This implies that the Schottky contacts are expected to be homogeneous, which is also confirmed from the ideality factor of the diode obtained from I–V characteristics at 300 K. The characteristic energy E_{00} is a property of the bulk semiconductor related to the transmission probability of the carrier through the barrier given by [20]:

$$E_{00} = \frac{h}{4\pi}\sqrt{\frac{N_A}{m * \varepsilon_S}} \quad (6)$$

N_A: carrier concentration whose value is 1.24×10^{17} cm^{-3} determined from the C–V measurements, h: Planck's constant, $m^* = 0.078m_o$, and $\varepsilon_s = 12.5\varepsilon_o$. The doping values affect directly the E_{00} values according to Eq. (6). The value of characteristic energy E_{00} is calculated to be 6.3 meV at 300 K. According to transport theory, since $E_{00} \ll kT$ (kT: thermal energy which is 25.8 meV at 300 K), thermionic emission is the dominating current mechanism at 300 K. The thermionic emission current permits a crossing over the barrier and dominates in semiconductors with weak doping $N_D < 10^{17}$ cm^{-3}.

In order to investigate the dependence of reverse current (I_R) of the Schottky contacts on the electric field (E), Frenkel–Poole and Schottky emission model are considered [21]. The plots of $\ln(I_R/E)$ and $\ln(I_R/T^2)$ versus $E^{1/2}$ are shown in Figs. 5 and 6. The Poole–Frenkel barrier lowering leads to the reverse leakage current given by

$$I_R \alpha E \exp\left(\frac{1}{kT}\sqrt{\frac{qE}{\pi\varepsilon}}\right) \quad (7)$$

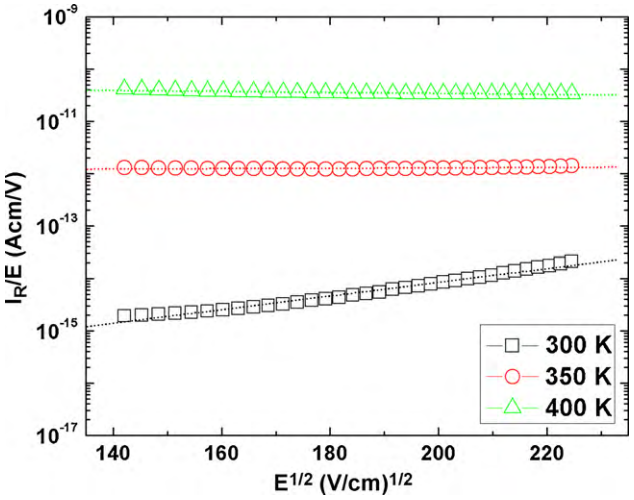

Fig. 5. Electric field dependence of Ti/p-type InP Schottky diode in reverse bias region: I_R/E versus $E^{1/2}$ plot for the Poole–Frenkel barrier lowering.

and the contribution to reverse current by Schottky lowering is given by

$$I_R \alpha T^2 \exp\left(\frac{1}{2kT}\sqrt{\frac{qE}{\pi\varepsilon}}\right) \quad (8)$$

where q: electronic charge, k: Boltzmann's constant, ε: permittivity and E: maximum electric field in the junction [22,23]. The plot gives the linear curve for the Frenkel–Poole and Schottky emission and the slope can be expressed as [21]:

$$S = \frac{q}{nkT}\sqrt{\frac{q}{\pi\varepsilon}} \quad (9)$$

where $n = 1$ for Frenkel–Poole emission and $n = 2$ for Schottky emission. The theoretically calculated slopes and the slopes obtained from the fits for both Frenkel–Poole emission and Schottky emission for different temperatures are represented in Table 2.

At 300 K, the slope determined from the fit to the data is slightly larger than the theoretical value for Frenkel–Poole emission. Therefore the result is more consistent with Frenkel–Poole emission and that the primary field enhanced carrier transport for the junction reverse current at 300 K is dominated by Poole–Frenkel barrier lowering in which the carrier transport from the metal into the conductive dislocation must occur via a trapped state rather than by direct thermionic emission from the metal [24]. In this mechanism, the defect states control the conduction. However, at 350 K and 400 K, the slopes determined from the fit are close to the theoretical value for Schottky emission. Thus, the result is more consistent with Schottky emission at 350 K and 400 K where the carrier absorbs thermal energy and then emitted over the potential barrier at the interface [24]. The electric field and temperature dependence of the current demonstrates a transition of the dependence of junction reverse current from Poole–Frenkel emission to Schottky emission as the temperature is elevated from 300 K to 400 K.

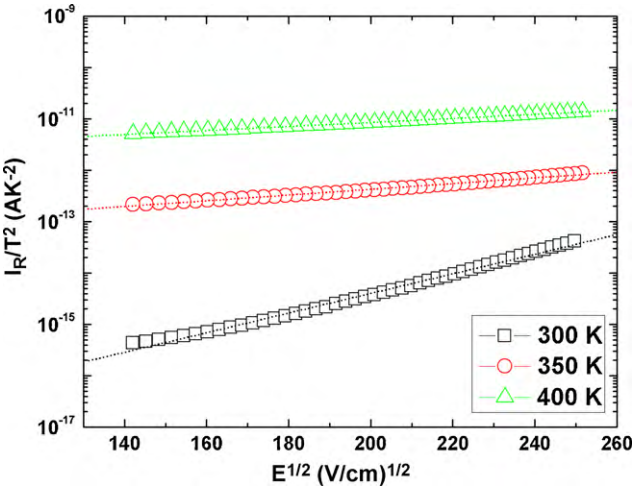

Fig. 6. Electric field dependence of Ti/p-type InP Schottky diode in reverse bias region: I_R/T^2 versus $E^{1/2}$ plot for the Schottky barrier lowering.

Table 2
The calculated and experimental values of Frenkel–Poole emission and Schottky emission values.

Temperature (K)	Frenkel–Poole emission $(V/cm)^{-1/2}$		Schottky emission $(V/cm)^{-1/2}$	
	Calculated	From the fit	Calculated	From the fit
300	0.0088	0.0130	0.0044	0.0190
350	0.0075	0.0038	0.0037	0.0055
400	0.0066	0.0094	0.0035	0.0039

4. Conclusions

The I–V characteristics of the Ti/p-type InP Schottky diode have been measured in the temperature range of 300–400 K. The diode showed a near ideal behavior with an ideality factor value of 1.08 at 300 K and deviates from ideality with increase of temperature. It is found that the barrier heights extracted from I–V characteristics increased with measured temperature in the range of 0.73–0.76 eV. The C–V characteristics of Ti/p-type InP Schottky diode have been measured at different frequencies at room temperature. At high frequencies, the capacitance is low since the interface states cannot follow the changes in the applied voltage. The barrier heights calculated from the C–V measurements increased with increasing frequency. The variation in the barrier height obtained from I–V characteristics at 300 K and C–V measurements at a frequency of 1 MHz at 300 K is negligible indicating the contacts to be more homogeneous. The diode showed the thermionic emission to be the dominating current transport mechanism at 300 K. The analysis of reverse current–voltage characteristics showed that reverse leakage current of the diode could be attributed to Poole–Frenkel barrier lowering at 300 K where the defect states control the conduction of current and due to Schottky barrier lowering at 350 K and 400 K. Schottky emission contributes to the conduction current as the temperature is elevated.

Acknowledgements

This work was supported by Priority Research Centers Program through the National Research Foundation of Korea (NRF) funded by Ministry of Education, Science and Technology of Korea (2009-0094033), and by the grant from the "Industrial Source Technology Development Programs (2009-F014-01)" of the Ministry of Knowledge Economy of Korea.

References

[1] K. Hattori, Y. Torii, Solid-State Electron. 34 (1991) 527–531.
[2] S.M. Sze, Physics of Semiconductor Devices, second ed., John Wiley & Sons, New York, 1981.
[3] R.T. Tung, Mater. Sci. Eng. R 35 (2001) 1–138.
[4] P. Victorovitch, P. Louis, M.P. Besland, A. Chovet, Solid-State Electron. 38 (1995) 1035–1043.
[5] S.Y. Zhu, R.L. Van Meirhaeghe, C. Detavernier, F. Cardon, G.P. Ru, X.P. Qu, B.Z. Li, Solid-State Electron. 44 (2000) 663–671.
[6] A. Gumus, A. Turut, N. Yalcin, J. Appl. Phys. 91 (2002) 245–250.

[7] B. Abay, G. Cankaya, H.S. Guder, H. Efeoglu, Y.K. Yogurtcu, Semicond. Sci. Technol. 18 (2003) 75–81.
[8] R. Hackam, P. Harrop, IEEE Trans. Electron Devices 19 (1972) 1231–1238.
[9] K. Ejderha, N. Yildirim, B. Abay, A. Turut, J. Alloys Compd. 484 (2009) 870–876.
[10] A. Singh, P. Cova, R.A. Masut, J. Appl. Phys. 76 (1994) 2336–2342.
[11] C.-Y. Wu, J. Appl. Phys. 51 (1980) 3786–3789.
[12] S. Aydogan, M. Saglam, A. Turut, Vacuum 77 (2005) 269–274.
[13] V. Janardhanam, A. Ashok Kumar, V. Rajagopal Reddy, P. Narasimha Reddy, J. Alloys Compd. 485 (2009) 467–472.
[14] P.A. Pipinys, A.K. Rimeika, V.A. Lapeika, A.V. Pipiniene, Semiconductors 35 (2001) 181–184.
[15] T. Funaki, T. Kimoto, T. Hikihara, IEICE Electron. Express 5 (2008) 198–203.
[16] F.A. Perez, A. Singh, G. Aroca, Proceedings of the 1998 Second IEEE International Caracas Conference on Devices, Circuits and Systems, 1998, pp. 79–82.
[17] E.H. Rhoderick, R.H. Williams, Metal–Semiconductor Contacts, second ed., Clarendon Press, Oxford, 1988.
[18] S. Asubay, O. Gullu, A. Turut, Vacuum 83 (2009) 1470–1474.
[19] C.W. Wilmsen, Physics and Chemistry of III–V Compound Semiconductor Interfaces, Plenum, New York, 1985.
[20] D.K. Schroder, Semiconductor Material and Device Characterization, third ed., John Wiley & Sons, Inc. Publication, New Jersey, 2006.
[21] H.D. Lee, IEEE Trans. Electron Devices 47 (2000) 762–767.
[22] A. Chatterjee, M. Rodder, I.C. Chen, IEEE Trans. Electron Devices 45 (1998) 1246–1252.
[23] C.H. Han, K. Kim, IEEE Electron Device Lett. 12 (1991) 74–76.
[24] J. Lin, S. Banerjee, J. Lee, C. Teng, IEEE Electron Device Lett. 11 (1990) 191–193.